Analysis of the Power Coupling Between an Antenna and a Device Under Test in a MSRC to Replace Onboard Immunity Tests of Automotive Equipment

Clovis Bule Mbo, Marco Klingler, Lionel Pichon, Mohamed Bensetti

Analysis of the Power Coupling Between an Antenna and a Device Under Test in a MSRC to Replace On-board Immunity Tests of Automotive Equipment

Clovis Bule Mbo[1,2], Marco Klingler[1]
[1]Stellantis, Centre technique de Vélizy, route de Gisy,
78943 Vélizy-Villacoublay,
clovis.bulembo@stellantis.com

Lionel Pichon[2], Mohamed Bensetti[2]
[2]Université Paris-Saclay, CentraleSupélec, CNRS,
Laboratoire de Génie Electrique et Electronique de Paris,
91192, Gif-sur-Yvette, France.
Sorbonne Université, CNRS, Laboratoire de Génie
Electrique et Electronique de Paris, 75252, Paris, France.
Lionel.pichon@geeps.centralesupelec.fr

Abstract— **This paper discusses the possibility of correlating radiated immunity test results obtained in a mode stirred reverberation chamber (MSRC), with results obtained when testing in near field the electronic and electrical automotive equipment immunity to on-board transmitters. This correlation is investigated experimentally using a device representative of an automotive embedded system over a ground plane in both cases. The device under test (DUT) is composed of a metallic box with patch antennas on its external surface. We perform comparisons between S-parameters measured between the test antenna and the patch antennas in the near field test (NFT) and in the MSRC. The purpose of this paper is to show that, the electromagnetic couplings on a DUT when testing its immunity to on-board transmitter in the NFT, are similar to the ones obtained in the MSRC but at a lower level. This comparison of S-parameters demonstrates that measurements performed in the MSRC can be sufficient to test the immunity of electrical and electronic equipment to on-board transmitters, if the power level applied during the test is increased.**

Keywords—EMC, RF, reverberation chamber, MSRC, anechoic chamber, On-board transmitter, radiated immunity.

I. INTRODUCTION

Nowadays, more and more electrical and electronic (EE) equipment are embedded in automotive vehicles. These equipment provide various functions from user comfort to safety on-board. Mobile phones and other communication devices or Personal Assistance Devices ("PADs") are possible sources of electromagnetic interferences when they are located near EE equipment. All embedded systems installed in vehicles are therefore tested unitarily in immunity on tables to various types of electromagnetic interferences. Among these tests, we distinguish the immunity tests to mobile on-board transmitters carried out according to the ISO 11452-9 standard [1]. The immunity tests to on-board transmitters consist in testing the equipment on a table by moving a representative transmitting antenna at a short distance around the DUT and its cable harnesses. The surfaces of the DUT are partitioned to cells of 100 x 100 mm and the transmitting antenna is placed at a distance of 50 mm to each cell of the DUT in two orthogonal orientations.

These components tests are performed by the equipment suppliers according to the internal standards of the car manufacturers, based on the international standards [1]. The new generations of radio-communication (in particularly 5G) introducing new frequency bands, today up to 6 GHz and eventually in a few years at even higher frequencies, requires an important extension of the immunity tests to the on-board transmitters in order to cover all new frequencies bands.

Electrical and electronic equipment can be tested unitarily on a table in immunity in the MSRC according to the ISO 11452-11 standard [2]. The immunity tests in MSRCs consist in placing the overall equipment and their cable harnesses in a strongly inhomogeneous electromagnetic environment.

The purpose of this paper is to demonstrate experimentally the equivalence between the results of the immunity tests on the on-board transmitters and those of the immunity tests in the reverberation chamber. A lot of work [3-6] has been done in the community to compare immunity tests performed in an MSRC with those performed in the anechoic chamber or in another electromagnetic test environment. In [4], a 3-axis electrical field probe is used inside a cubic metallic box with a slot in order to measure the maximum of a rectangular component of the E-field in the MSRC and in the semi-anechoic chamber (SAC) in the 200 -1000 MHz frequency range. The results depend on the orientation of the slot on the metallic box. In the last few years, other comparisons have been done for wireless communication testing [5,6]. Measurements in the SAC are generally performed with the transmitting antenna at least 1m of the DUT. It is possible to calculate the difference between the field intensity radiated inside a CSA by a transmitting antenna located at least one meter from the location of the equipment to be tested and the field intensity radiated inside an MSRC with equal incident power in both cases. when the CSA tests are performed in near field it is not possible to calculate this difference.

The method that we propose consists in comparing S-parameters measured with a transmitting antenna located near the DUT and those measured in the MSRC. The principle of the method consists in measuring the electromagnetic coupling between a transmitter antenna and several patch antennas positioned on the external surface of the DUT above a ground plane table. Thus, we can compare the maximum received power on the DUT when the transmitting antenna is located at 50 mm around the DUT and the maximum received power on the DUT in the MSRC. In the MSRC, the position of the transmitting antenna avoids any line of sight coupling with the DUT. We will be interested in the maximum received powers on the DUT in order to compare only the worst cases of the DUT immunity in each test environment.

This paper is organized as follow; Section II describes the DUT, and the transmitting antenna used. Section III presents the theoretical aspects of the coupling in NFT and in the MSRC. We present in section IV, the measurements setups for near field tests and in MSRC, and we discuss couplings measurement results when operating as usually performed for

immunity test to on-board transmitters and when operating in the MSRC. We then conclude in the section V.

II. DESCRIPTION OF THE DEVICE OF THE TEST

In order to carry out measurements of electromagnetic field couplings on any equipment in different test environments, we first designed a DUT, which represents the embedded equipment in the vehicle. This DUT consists of a parallelepiped metallic box of 50 x 100 x 200 mm, on which patch antennas with a U-shaped slot are installed on the external faces. Each patch antenna on the DUT is feeding using a coaxial probe which outer conductor is connected to the bottom at the ground plane and the inner conductor extends through the dielectric and is soldered to the radiated patch.

Each of the six faces of the metallic box has two patch antennas installed. One is horizontally polarized and the other vertically polarized. The metallic box has three pairs of faces with the same size. The two patch antennas on each opposite side are oriented in such a way to avoid rotational mirroring.

The patch antennas are located on the metallic box as shown in figure 1. They all have the same dimensions ($L_p = 38$ mm and $W_p = 44$ mm), identical characteristics and are matched in the 2.5 to 4 GHz frequency band with a maximum gain around 7 dB.

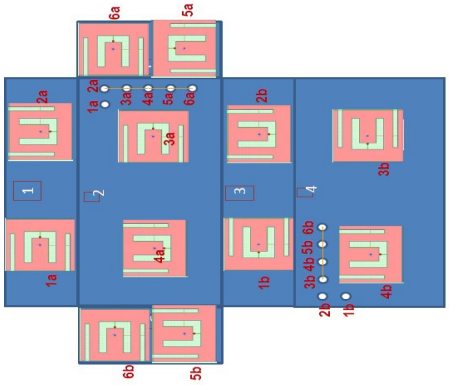

Figure 1: Schematic view of the DUT.

To simulate the portable transmitter (source of the electromagnetic disturbance), a small Biconical broadband antenna SBA 9119 is used [1]. It is designed for wide bandwidth and for immunity tests in the close distance to the DUT. The SBA 9119 antenna is matched in the 1 to 6 GHz frequency band, in which it has an isotropic gain around 0 dB.

S-parameters and the gains of antennas have been measured in the free space for one patch antenna and for the SBA 9119 antenna. These measurements have been compared to the simulation results and will be presented in this paper in the next section.

III. THEORETICAL APPROACH

The coupling between the transmitting antenna (Tx) and the receiving patch antennas (Rx) on the DUT is studied through the measurement of the power balance between Tx and Rx antennas in the NFT and in the MSRC using a vector network analyzer (VNA).

Let us assume that the Tx and Rx antennas as shown in figure 2 are neither perfectly matched nor perfectly efficient.

The injected power (P_{inj}) from the internal generator of the VNA on the port 1 and the measured power (P_{meas}) from the receiving antenna on the port 2 are written:

$$P_{inj} = \frac{P_t}{(1-|S_{11}|^2)G_t} \quad (1)$$

$$P_{meas} = P_r(1-|S_{22}|^2)G_r \quad (2)$$

where S_{11} and S_{22} include backscattering effects. G_t and G_r are respectively the transmitting and receiving antenna gains. The transmitted power P_t is the power radiated by Tx. And the received power P_r is the power received by Rx.

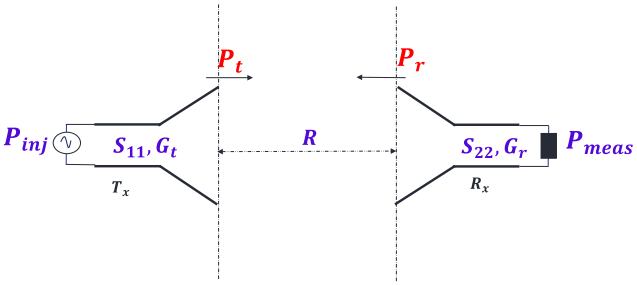

Figure 2: Two antennas separated by a distance R

If Tx and Rx are lossless and perfectly matched, then P_t and P_r are respectively equals to P_{inj} and P_{meas}.

The S_{21}- parameter, the power at the receiving terminal and the power injected are related by:

$$(|S_{21}|^2) = \frac{P_{meas}}{P_{inj}} \quad (3)$$

A. Power balance in free space

In free space, the Friis transmission equation is commonly used to calculate the received power from a Rx, when transmitted from a Tx, separated by a distance R> $\frac{2D^2}{\lambda}$ [7], where D is the largest dimension of either antenna, and λ is the wavelength.

In this paper, the distance R is equal to 50 mm and is below $\frac{2D^2}{\lambda}$. Therefore, the transmitter is in the near field region and Friis equation does not remain valid. However, the received power can be computed using numerical simulation with a 3D software solving Maxwell equations.

Figure 3 shows the 3D configuration of the measurement set up in the free space.

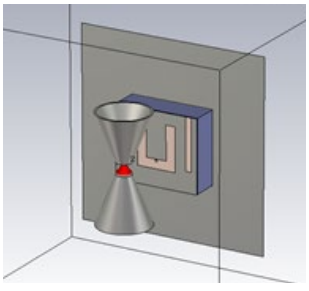

Figure 3: Numerical model of the problem

In order to confirm measurement results, measurements and simulations of the S-parameters and gains of a receiving

patch antenna and the SBA 9119 transmitting antenna have been compared.

In figures 4 and 5, we observe that there is a good agreement between measurements and simulations. The average discrepancy between measurements and simulations of the S_{11}-parameters is around 0.9 dB for the patch antenna and 1 dB for the SBA 9119 transmitting antenna .

The average discrepancy between measurements and simulations of the gains for the patch and the transmitting antennas are respectively 1.3 dB and 0.6 dB.

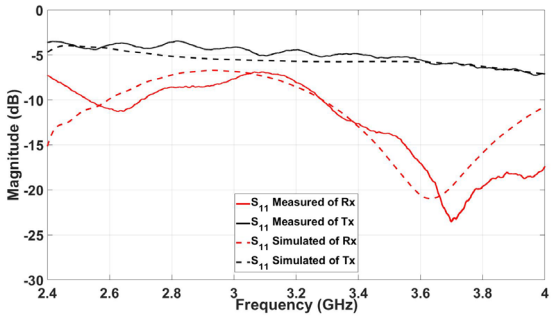

Figure 4:Tx and Rx S_{11}-parameters comparison

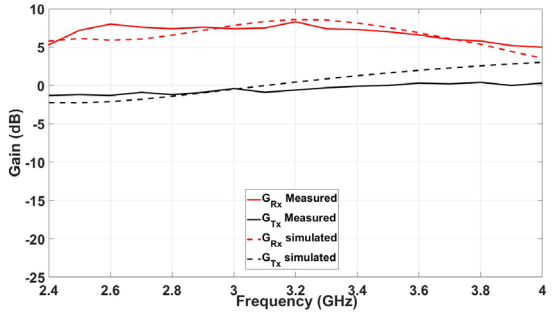

Figure 5: Gains of transmitting and receiving antennas

We also obtained similar results between simulation and measurements of the coupling between the transmitting antenna and one receiving patch antenna in the free space as shown in the figure 6. The average discrepancy between measurement and simulation is around 0.9 dB.

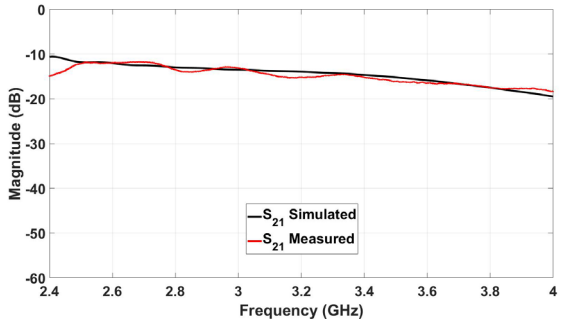

Figure 6: S_{21} parameters comparison in free space

The differences between numerical models and measurements can be due to the difference between material characteristics used in the numerical model and those existing in reality. Some differences may also be due to approximated dimensions, or missing excitation details in the numerical simulation. However, this numerical model allows us to confirm measurement results in free space.

B. Power balance in MSRC

In [8], it is shown that the average received power on the DUT in the MSRC is the product of the scalar power density and the effective area of an isotropic antenna. This average power is calculated on a sample of the measurements made during the rotation of the mode stirrer.

$$\langle P_r \rangle = \frac{1}{2}\frac{\langle |E_t|^2 \rangle}{\eta}\frac{\lambda^2}{4\pi} = \frac{(<\mathrm{P_{meas}}>)}{(1-|(<\mathrm{S_{22}}>)|^2)\mathrm{G_r}} \quad (4)$$

where $\frac{\langle |\boldsymbol{E_t}|^2 \rangle}{\boldsymbol{\eta}}$ is the scalar power density expressed in terms of the total root means squared electric field $\boldsymbol{E_t}$ and the wave impedance of the free space $\eta = 120\pi$.

The term $\frac{\boldsymbol{\lambda^2}}{\boldsymbol{4\pi}}$ is the effective area of an isotropic antenna. The symbol $\langle\,\rangle$ is used to indicate the mean value of the quantity over the different positions of the stirrer.

The received power on a DUT is also function of the quality factor of the chamber. The quality factor Q is defined as the ratio between the average energy over all states of the chamber completed during the stirring process and the power dissipated in the elements inside the chamber. [9].

$$\mathrm{Q} = \frac{\omega \mathrm{U}}{\mathrm{P_d}} = \frac{\omega\varepsilon<E_t^2>\mathrm{V}}{<\mathrm{P_t}>} \quad (5)$$

where U is the energy stored in the cavity, $\mathrm{P_d}$ is the dissipated power in the chamber and is equal to the average transmitted power, V is the volume of the chamber, ε is the permittivity and ω is the angular frequency.

$$\mathrm{Q} = \frac{\omega\varepsilon<E_t^2>\mathrm{V}}{(1-|<\mathrm{S_{11}}>|^2)\mathrm{G_t}P_{inj}} \quad (6)$$

Starting from (4) and (6), we obtain:

$$E_t^2 = \frac{Q(1-|<\mathrm{S_{11}}>|^2)\mathrm{G_t}P_{inj}}{\omega\varepsilon V} = \frac{2\eta}{\frac{\lambda^2}{4\pi}}\frac{<(\mathrm{P_{meas}})>}{(1-|<\mathrm{S_{22}}>|^2)\mathrm{G_r}} \quad (7)$$

Thus S_{21} and $<\mathrm{P_{meas}}>$ are given by:

$$<\mathrm{P_{meas}}> = P_{inj}\frac{\mathrm{Q}\frac{\lambda^2}{4\pi}}{2\eta\omega\varepsilon V}(1-|<\mathrm{S_{11}}>|^2)\,(1-|<\mathrm{S_{22}}>|^2)\mathrm{G_rG_t} \quad (8)$$

$$<|S_{21}|^2> = \frac{\mathrm{Q}\frac{\lambda^2}{4\pi}}{2\eta\omega\varepsilon V}(1-|<\mathrm{S_{11}}>|^2)\,(1-|<\mathrm{S_{22}}>|^2)\mathrm{G_rG_t} \quad (9)$$

The walls, antennas and other elements inside the chamber contribute to the dissipation of energy in the cavity and to the value of the total quality factor.

$$\frac{1}{Q_{total}} = \frac{1}{Q_{walls}} + \frac{1}{Q_{Tx}} + \frac{1}{Q_{Rx}} + \frac{1}{Q_{DUT}} + \frac{1}{Q_{Stirrer}} + \frac{1}{Q_{others}} \quad (10)$$

At high frequencies, the total quality factor of the empty chamber with only antennas is mainly determined by the quality factor of the chamber walls [10].

In this paper, the theoretical expression of $<S_{21}>$ is calculated using the factor quality Q of the chamber walls.

$$Q_{walls} \cong \frac{3V}{2\mu_r S\delta_{walls}} \quad \text{with} \quad \delta_{walls} = \sqrt{\frac{2}{\omega\mu\sigma}} \quad (11)$$

where S is the internal surface of the chamber, δ_{walls} is the skin depth of the walls, σ is the electrical conductivity of walls and μ is the magnetic permeability of the walls.

The figure 7 shows the theoretical estimation of the quality factor of the chamber walls calculated according to (11). Usually, these predictions yield values five or ten times higher than the measured quality factors. These discordances are mainly due to the losses in the gaskets of the wall assembly, whose contribution is obviously omitted in (11) [10].

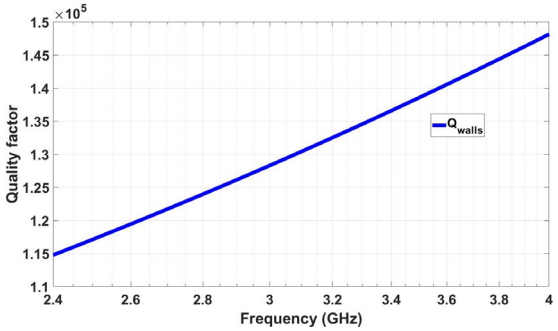

Figure 7: Theoretical quality factor of the chamber with dimensions: 3.25x4.11x4.96

The calculated S_{21}-parameters in the MSRC will be presented with measurements results in the next section.

IV. Experimental Measurements

Measurements of the S-parameters were performed in the frequency domain with a 9 kHz – 8.5 GHz VNA. Port 1 of the VNA is connected to the transmitting antenna while port 2 is connected to one of the patch antennas, both by means of coaxial cables and adequate interfaces. The calibration is performed at the output connector of cables intended to be plugged in the input connectors of the antennas.

A. Coupling measurements in the NFT

As shown in Figure 8, the setup of the table test is composed of a transmitting antenna and a ground plane table where the DUT is placed at 50 mm above the ground plane. According to [1], all surfaces of the DUT that are to be tested, shall be divided into square areas of 100 x 100 mm. The transmitting antenna shall be placed at a distance of 50 mm from the surface of the DUT, and the center of each area shall be exposed to the center of the transmitting antenna, in the two orthogonal orientations. In this paper the S_{21}-parameters were measured between the transmitting antenna and each of patch antennas of the metallic box, as shown in the figure 9. Measurements as performed in the SAC requires the rotation of the DUT in order to test all the six faces. Otherwise, the face on the bottom of the DUT cannot be tested.

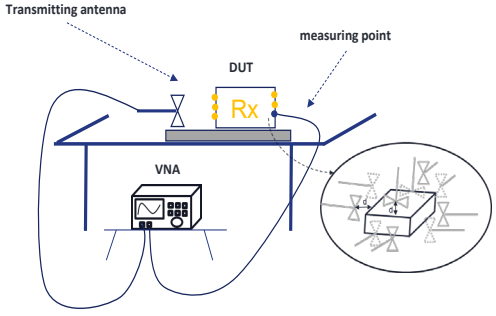

Figure 8: experimental approach in the NFT

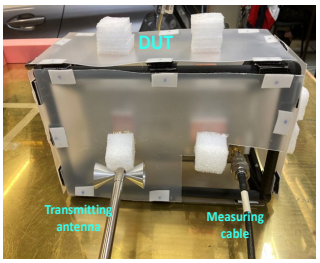

Figure 9: Test set up above a ground plane table in the NFT

As shown in figure 10, when the transmitting antenna elements have the same orientation than the U slot of the patch antenna, the antennas polarizations are matched. In this case, the coupling is maximum. The coupling is negligible when the transmitting antenna and the U slot of the patch antenna have crossed orientations.

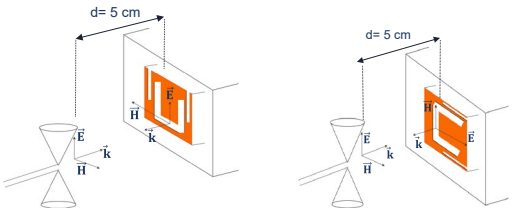

Figure 10: Transmitting and receiving antennas orientations

We presented in this paper, only the coupling results for cases where the transmitting antenna has the same orientation as the U slot on patch antennas.

The patch antennas on the DUT are not perfectly matched. We quantified their reflected powers by measuring S_{11} -parameters and calculating the voltage standing wave ratio (VSWR) of each patch antenna. As shown in figure 11, in the 2.4 to 4 GHz frequency range the VSWR of patch antennas goes from 1 to 3. The patch antennas are reflecting up to 25% of measured power. The reflected powers of patch antennas on the DUT will be different from one patch to another.

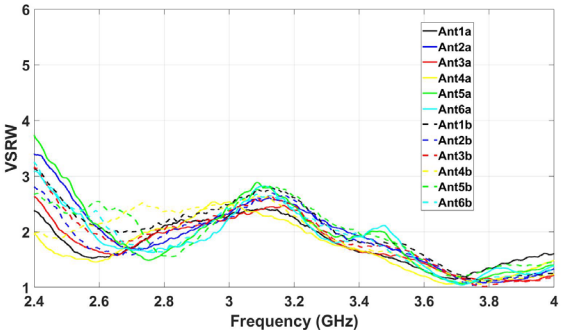

Figure 11:Measured VSWR of patch antennas on the DUT

The maximum couplings between the transmitting antenna and each patch antenna on the DUT are shown in figure 12. The measurement results on the DUT depend on the antenna gains and on the impedance mismatch of each patch antenna. It can be seen that there is a dispersion of the measurements. It is around, 8 dB at 2.4 GHz and 4 dB at 4 GHz. This dispersion is mainly due to the dispersion of the reflected powers on patch antennas

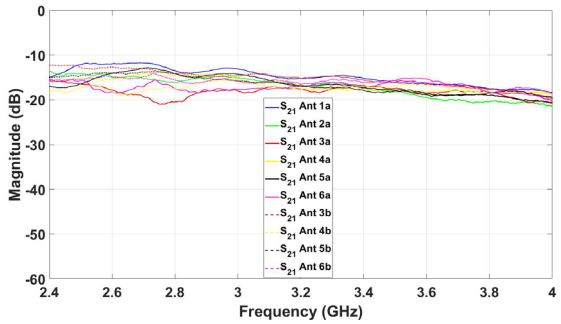

Figure 12: Maximum values of S_{21} between the transmitting antenna and patch antennas of the box, in the NFT

B. Coupling measurements on table in MSRC

Measurements were carried out in the Stellantis reverberation chamber. It is a 3.25 x 4.11 x 4.96 m shielded room, including a mechanical stirrer. The experimental approach consists in measuring the S-parameters of a system composed of the SBA 9119 transmitting antenna and the patch antennas of the DUT over a full revolution of the stirrer. The experimental approach is represented in figure 13.

We place the DUT at 50 mm above the table ground plane, as shown in figure 14. For each frequency, we collected the S-parameters carried out on 12 positions of the stirrer.

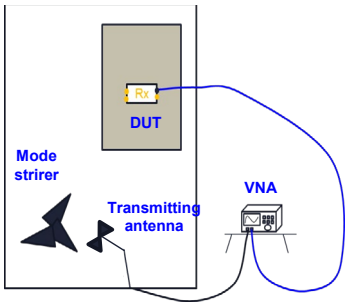

Figure 13: Experimental approach in the MSRC

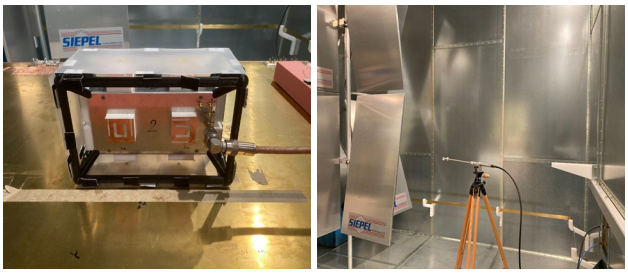

Figure 14: Test set up on the table in the MSRC

Figure 15 shows the maximum couplings between the transmitting antenna and each patch antenna on the DUT over all the 12 positions of the stirrer, except for those faced bottom (Ant1b and Ant2b). It also shows the theoretical estimation of the S_{21}-parameters calculated according to (9). The difference between the measurement results and the theoretical results is due to the differences between the theoretical quality factor and the effective measured quality factor.

In the MSRC, the couplings on the DUT are independent of the orientations of the patch antennas on the DUT. Couplings are identical on all the patch antennas on the DUT.

For the patch antennas faced bottom, as shown in the figure 16, we observe a small increase and decrease of the couplings respectively around 2.7 GHz and 3 GHz. In the MSRC, the DUT is exposed to the statistically uniform field distribution in the test volume of the chamber. Close to electrically conductive walls or ground plane, the tangential electric field is zero and therefore the total electric field near the ground plane is lower than the total field far the ground plane [11], [12]. The ISO 11452-11 standard [2] recommends to place the DUT at least d> λ/4 from the conductive walls. In this case, the bottom base of the DUT is at 25 mm above the ground plane of the test table. This distance is appropriate for tests on frequencies above 3 GHz. For frequencies between 2.4 and 3 GHz, the 25 mm distance is smaller than λ/4.

One of the advantages of the measurements in the MSRC is that there is no need to rotate the transmitting antenna around the DUT. If the DUT is above a table without ground plane, measurements as performed in the MSRC do not require the rotation of the DUT in order to test the face on the bottom of the DUT. It allows to perform measurements without altering measurement conditions.

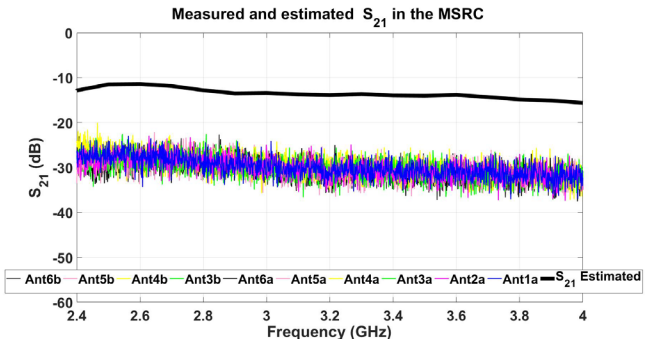

Figure 15: Maximum value of S_{21} between the transmitting antenna and patch antennas on the DUT in the MSRC

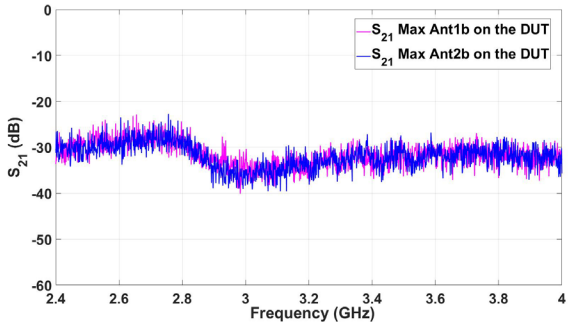

Figure 16: Maximum value of S_{21} on the surface of the bottom of the box in the MSRC

C. Comparison of coupling measurements in the NFT and in the MSRC

Figure 17 shows the comparison between coupling measurements on a DUT in the NFT and the coupling measurements in the MSRC. It can be seen that couplings on the DUT in the NFT with transmitting antenna placed at a distance of 50 mm from the patch antennas are around 10 dB higher than couplings in the MSRC over all the frequency band 2.4 – 4 GHz.

In the NFT, the couplings between a transmitting antenna and the patch antennas on the DUT are proportional to the distance between them. If the distance of 50 mm used for

testing changes, the 10 dB difference between the transmission coefficients will change to another value.

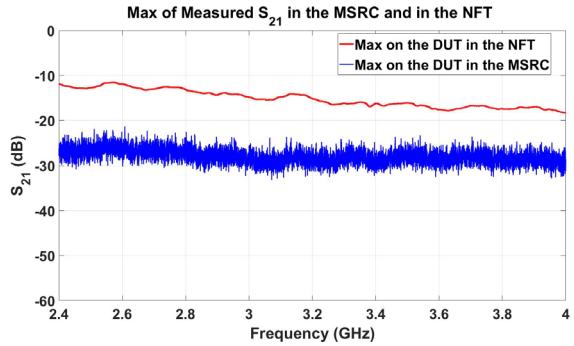

Figure 17: Comparison between measurement in the NFT and in the MSRC

This comparison highlights the possibility to reach the same levels of couplings on a DUT in the MSRC as in the NFT with transmitting antenna placed at a distance of 50 mm from the patch antennas. We need a power ten times higher in the MSRC than on the NFT.

V. Conclusion

In this paper, we investigated an experimental comparison between electromagnetic couplings on a device above a ground plane in the SAC and in the MSRC. A particular DUT representative of an embedded automotive equipment was designed. It consists of a metallic box having two patch antennas on each face in order to measure the electromagnetic coupling. Measurements were performed both above a ground plane table in the NFT as for the on-board transmitter immunity tests, and in a reverberation chamber, as for the classical immunity tests.

For the NFT tests as well as for the MSRC tests, we used the same transmitting antenna and the same DUT above a ground plane; in order to compare only the test environment effects, both tests are performed under identical conditions changing only the position of the transmitting antenna according to the tests performed in NFT or MSRC.

The results obtained in this paper mainly depends on the distance between the DUT and the transmitting antenna for the NFT tests and on the physical and geometrical characteristics of the MSRC.

The electromagnetic coupling in the reverberation chamber, resulting from random field's distribution, leads to lower levels of transmitted power than those obtained by placing the transmitting antenna at 50 mm from the DUT. However, increasing the incident power in the chamber, allows to obtain similar received power on the DUT and then the same conclusions about the level of immunity.

As for the results of S-parameters measures, it was found out that the ratio of the received power on the DUT above a ground plane table in the NFT to that in the MSRC is about 10. Therefore, the immunity of the automotive equipment to the on-board transmitters can be tested in the MSRC increasing reasonably the input power.

The required power in MSRC will thus be equal to the product of the test power in NFT by the ratio between the S_{21}-parameters measured in NFT and in MSRC as in (12) and (13).

So, to find out the required power for MSRC tests without repeating the NFT measurements, we propose to perform power calibration measurements. The power calibration measurements consist in measuring the S_{21} -parameters between the transmitting antenna and a calibration receiving antenna in the NFT, and in the MSRC

$$\Delta_{S21} = \frac{(S_{21})_{NFT}}{(S_{21})_{MSRC}}, \tag{12}$$

$$\left(P_{inj}\right)_{MSRC} = \left(P_{inj}\right)_{NFT} \times \Delta_{S21} \tag{13}$$

Automotive equipment are usually tested with their harnesses cables. In order to propose a new method for testing immunity to on-board transmitters in the MSRC, future work will investigate comparison between couplings on the harnesses cables of automotive equipment ,in the NFT as for immunity to on-board testing and in the reverberation chamber as for the classical radiated immunity test

References

[1] ISO 11452-9 Road vehicles – Component test methods for electrical disturbances from narrowband radiated electromagnetic energy - Part 9: Portable transmitters

[2] ISO 11452-11 – Road vehicles - Component test methods for electrical disturbances from narrowband radiated electromagnetic energy - Part 11: Reverberation chamber

[3] E. Amador, "A Probabilistic Approach to Susceptibility Measurement in a Reverberation Chamber," in Asia Pacific Symposium on EMC, Singapore, May 2012.

[4] K. Slattery and J. Neal, "A comparison of reverberation chamber and semi-anechoic chamber testing for automotive susceptibility," Gateway to the New Millennium. 18th Digital Avionics Systems Conference. Proceedings (Cat. No.99CH37033), 1999.

[5] F. Alhorr, M. Wiles, S. Fermiñán-Rodríguez and C. Wehrmann, "On the comparison between anechoic and reverberation chambers for wireless OTA testing," 2013 7th European Conference on Antennas and Propagation (EuCAP), 2013, pp. 1852-1856.

[6] P. Kildal and A. A. Glazunov, "OTA testing of 3G-5G devices with MIMO: From anechoic chambers to reverberation chambers and … back again?," 2017 IEEE International Symposium on Antennas and Propagation & USNC/URSI National Radio Science Meeting, 2017, pp. 1697-1698,

[7] Constantine A. Balanis, Antenna Theory, New Jersey: A John Wiley &Sons, 2005.

[8] D. A. Hill, "Plane Wave Integral Representation for fields in the reverberation chamber," IEEE transactions on electromagnetic compatibility, vol. 40, no. 3, AUGUST 1998.

[9] P. Besnier, C. Lemoine and J. Sol, "Various estimations of composite Q-factor with antennas in a reverberation chamber," 2015 IEEE International Symposium on Electromagnetic Compatibility (EMC), 2015, pp. 1223-1227

[10] P. Besnier and B. Demoulin, Electromagnetic Reverberation Chambers. ISTE/Wiley, 2011.

[11] D. A. Hill, "Boundary fields in reverberation chambers," in IEEE Transactions on Electromagnetic Compatibility, vol. 47, no. 2, pp. 281-290, May 2005.

[12] M. Magdowski and D. A. Hill, "Corrections to "Boundary Fields in Reverberation Chambers" [May 05 281-290]," in IEEE Transactions on Electromagnetic Compatibility, vol. 51, no. 2, pp. 420-421, May